Stratigraphic, sedimentological, geochemical, mineralogical and geochronological data characterizing the Upper Miocene sequence of the Turiec Basin, Western Carpathians (Central Europe)

Michal Šujan, Kishan Aherwar, Rastislav Vojtko, Régis Braucher, Katarína Šarinová, Andrej Chyba, Jozef Hók, Anita Grizelj, Radovan Pipík, Bronislava Lalinská-Voleková, et al.

Data in Brief 52 (2024) 109810

Contents lists available at ScienceDirect

Data in Brief

journal homepage: www.elsevier.com/locate/dib

Data Article

Stratigraphic, sedimentological, geochemical, mineralogical and geochronological data characterizing the Upper Miocene sequence of the Turiec Basin, Western Carpathians (Central Europe)

Michal Šujan[a,*], Kishan Aherwar[a], Rastislav Vojtko[a], Régis Braucher[b], Katarína Šarinová[c], Andrej Chyba[d], Jozef Hók[a], Anita Grizelj[e], Radovan Pipík[f], Bronislava Lalinská-Voleková[g], Barbara Rózsová[a], Aster Team[b]

[a] *Department of Geology and Paleontology, Faculty of Natural Sciences, Comenius University in Bratislava, Ilkovičova 6, 842 15 Bratislava, Slovakia*
[b] *CNRS-IRD-Collège de France-INRA, CEREGE, Aix-Marseille Univ., 13545 Aix-en-Provence, France*
[c] *Department of Mineralogy, Petrology and Economic Geology, Faculty of Natural Sciences, Comenius University in Bratislava, Ilkovičova 6, 842 15 Bratislava, Slovakia*
[d] *Institute of Chemistry, Slovak Academy of Sciences, Dúbravská cesta 9, 845 38 Bratislava, Slovakia*
[e] *Croatian Geological Survey, Sachsova 2, 10 000 Zagreb, Croatia*
[f] *Earth Science Institute, Slovak Academy of Sciences, Ďumbierska 1, Banská Bystrica SK-97411, Slovakia*
[g] *SNM-Natural History Museum, Vajanského náb. 2, P.O. BOX 13, 810 06 Bratislava, Slovakia*

A R T I C L E I N F O

Article history:
Received 14 August 2023
Revised 8 November 2023
Accepted 9 November 2023
Available online 17 November 2023

Dataset link: Data for stratigraphic, granulometric, geochemical and authigenic 10Be/9Be geochronological analysis of Upper Miocene outcrops in the Turiec Basin, Western Carpathians (Central Europe) (Original data)

A B S T R A C T

The data included in this article specify the characteristics of the Upper Miocene fill of the Turiec Basin and served for reconstruction of temporal evolution of depositional systems in this intermontane basin located within the Western Carpathians (Central Europe). The borehole lithological log data were used to describe the stratigraphy of the Turiec Basin in geological sections and were gained in the Geofond archive of the State Geological Institute of Dionýz Štúr. The sedimentological data were acquired by field research applying facies analysis to nine outcrop sites. The outcrops served for grain size analyzes performed by sieving and laser

* Corresponding author.
E-mail address: michal.sujan@uniba.sk (M. Šujan).

https://doi.org/10.1016/j.dib.2023.109810

Keywords:
Facies analysis
Lake regression
Intermontane basin
Paleoenvironment
Cosmogenic nuclides
Authigenic 10Be/9Be dating

diffraction, for geochemical analyzes using ICP-ES, ICP-MS and XRF, and for mineralogical analyzes of whole rock and clay fraction by XRD. Moreover, the muddy layers on outcrops served for collection of 31 samples for the authigenic $^{10}Be/^{9}Be$ dating. The geochronological data are presented by using five different initial ratios for calculation, determined within the Turiec Basin at the Late Pleistocene alluvial fan and river terrace sites as well as at two Holocene muddy floodplain sites. Another initial ratio data are gained from an Upper Miocene lacustrine succession dated independently by magnetostratigraphy in previous research. Finally, a summary of previously published strontium isotope data from the Turiec Basin is included. The interpretations of the data are provided in Šujan et al., (2023) *Palaeogeography, Palaeoclimatology, Palaeoecology* 628, 111746.

Specifications Table

Subject	Geology
Specific subject area	Evolution of a Late Miocene intermontane long-lived lake, its dating and paleoenvironmental research
Data format	Raw and analyzed
Type of data	Table, Image, Graph, Figure
Data collection	Borehole lithological logs were acquired in the Geofond archive of the State Geological Institute of Dionýz Štúr from the archival reports. Boreholes were selected based on the stratigraphic thickness penetrated and location nearby the outcrops studied in detail. Sedimentological data were obtained using facies analysis on outcrops of the Upper Miocene succession within the Turiec Basin. The field research was performed in the years 2020–2022. Granulometric data were obtained by wet sieving in the case of gravelly sediment, and by laser diffraction using Malvern Mastersizer 3000 facility. Gravel sample clast images were taken using digital camera. Geochemical data were obtained by ICP-ES (major oxides) and ICP-MS (trace elements), and by XRF. The content of TOC, C and S was analyzed by the LECO Carbon-Sulphur analyzer. The beryllium isotopic data were obtained by ICP-MS measurements of total beryllium content in aliquots taken from the leaching solution, and by $^{10}Be/^{9}Be$ isotopic measurements using accelerator mass spectrometry. Sr isotope data were summarized by a literature review.
Data source location	Borehole lithological logs are secondary data acquired in the Geofond archive of the State Geological Institute of Dionýz Štúr (Mlynská dolina 3962/1, 817 04 Bratislava, Slovakia) from the archival reports, which are available online: https://da.geology.sk/navigator/?desktop=PublicThe studied outcrops are located in the Turiec Basin (Western Carpathians, Central Europe) with the following coordinates (latitude, longitude): • Ondrašová: 18.806°N; 48.941°E • Slovany: 18.821°N; 48.976°E • Valča: 18.838°N; 49.009°E • Socovce: 18.859°N; 48.950°E • Abramová – Kolísky: 18.786°N; 48.930°E • Blažovce: 18.849°N; 48.937°E • Turčiansky Peter: 18.893,49.036°E • Kúdel: 18.968°N; 49.119°E • Martin – claypit: 18.895°N; 49.065°E
Data accessibility	Repository name: Mendeley Data Data identification number: 10.17632/sdvpm9mf6m.5 Direct URL to data: https://data.mendeley.com/datasets/sdvpm9mf6m/5

(*continued on next page*)

Related research article M. Šujan, K. Aherwar, R. Vojtko, R. Braucher, K. Šarinová, A. Chyba, J. Hók, A. Grizelj, R. Pipík, B. Voleková, B. Rózsová, AsterTeam, Application of the authigenic $^{10}Be/^{9}Be$ dating to constrain the age of a long-lived lake and its regression in an isolated intermontane basin: The case of Late Miocene Lake Turiec, Western Carpathians, Palaeogeography, Palaeoclimatology, Palaeoecology 628 (2023), 111746, 10.1016/j.palaeo.2023.111746

1. Value of the Data

- The dataset provides a robust base for interpretation of evolution of depositional systems during the Late Miocene in the Turiec Basin, which is an important archive of paleogeographic changes in the central part of the Western Carpathians.
- The data obtained by multidisciplinary approach, combining sedimentological, paleoenvironmental and geochronological research, might serve for reconstructions of drainage network evolution in the orogenic belt.
- The dataset yields important clues to temporal variability in sediment supply to accommodation rate ratio caused by changes in geodynamic regime in the region.
- The authigenic $^{10}Be/^{9}Be$ dating in an intermontane basin yields promising results for future application of the method in similar settings.
- The data could be re-used for alternative interpretations of the basin evolution.

2. Data Description

This article describes the dataset of the linked repository [1], which is associated to the research paper focused on the Late Miocene evolution of the intermontane Turiec Basin in the Western Carpathians (Central Europe) [2] (Fig. 1A–C). The structure of the text follows the folder structure of the linked repository and refers to the files included in the repository [1].

2.1. Stratigraphic data based on geological sections of borehole logs

A set of 45 lithological profiles was acquired from the original reports of various geological surveys (listed in file “List of final reports including the boreholes used for the geological sections.xlsx”), and the lithology discovered by these boreholes is depicted in the geological sections in Figs. 2–4 (files “Geological section A–E.jpg”). The criteria used to distinguish facies associations in borehole logs, based on the facies analysis in [2], are explained in the file “List of criteria applied to establish facies associations in boreholes, in Šujan et al. (2023) Plaeogeography, Palaeoclimatology, Palaeoecology 628, 111746 boreholes.xlsx”. The explanations of borehole logs in Fig. 5 (file “Explanations to the geological sections.jpg”) include 15 different lithological classes present in the available logs. The geological sections A–D (Figs. 2,3) are located on the northern margin of the southern depocenter of the Turiec Basin (Fig. 1D), while the Section E (Fig. 4) displays basin fill of the northern depocenter (Fig. 1E). The geological sections (Figs. 2–4) show lateral and vertical trends in distribution of the lithological classes, which was used in [2] to establish a stratigraphic model of the Turiec Basin.

2.2. Sedimentology on outcrops

The facies analysis of nine outcrops in the Turiec Basin (location in Fig. 1C) led to a description of 27 distinct lithofacies, associated with specific depositional processes (file “List of lithofacies documented on the outcrops in the Turiec Basin.xlsx”). The vertically extensive exposures of alluvial fan deposits allowed a quantitative evaluation of the lithofacies distribution in

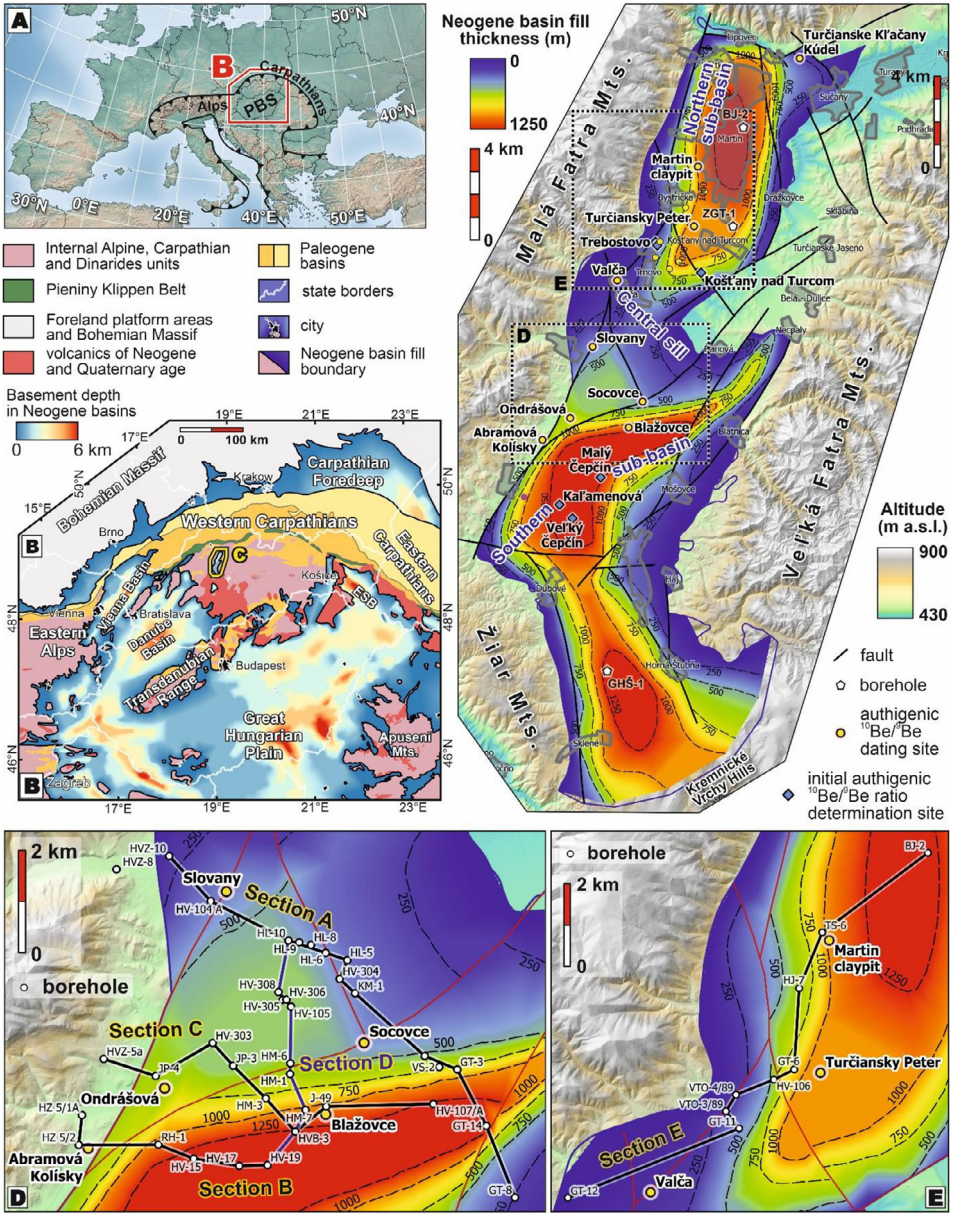

Fig. 1. Location of the Turiec Basin, studied in [2]. A: Location within the Alpine-Carpathian orogen in Central Europe. B: The Turiec Basin is placed in the Central Western Carpathians. The map is modified from [3]. C: Location of the studied sites of the Turiec Basin together with the thickness of the Neogene basin fill and Lidar DEM topography of the mountains surrounding the basin. The map is modified from [2]. Isobaths based on [4]. The Lidar DEM data were provided by the Geodesy, Cartography and Cadaster Authority of the Slovak Republic. D–E: Location of the geological sections in Figs. 3–5. The maps are modified from [2]. Dating sites description and sample abbreviations: alluvial fans – Ondrašová (Ondr), Slovany (Slov), Valča (Val); braided river – Socovce (SocKos), Abramová – Kolísky (Kolisky); fan delta – Blažovce (Blaz); open lake – Martin – claypit (MarTeh), Turčiansky Peter (TurPet), Turčianske Kľačany – Kúdel (Kudel).

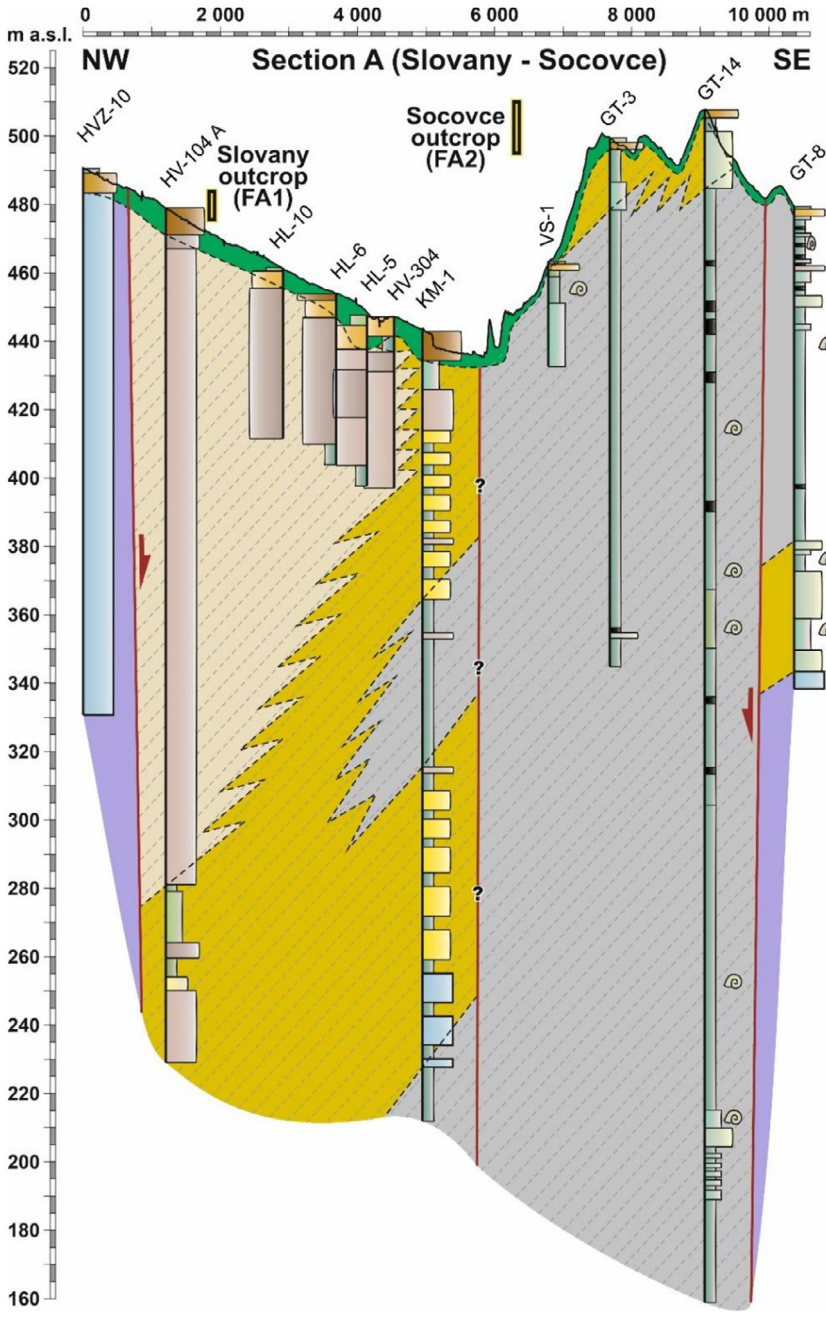

Fig. 2. Geological section depicting borehole lithological profiles along the line between Slovany and Socovce outcrops. The position of the outcrops is a projection perpendicular to the section line preserving the altitude of the stratigraphic section. A simplified version of the section is present in [2]. Explanations in Fig. 5. Location in Fig. 1.

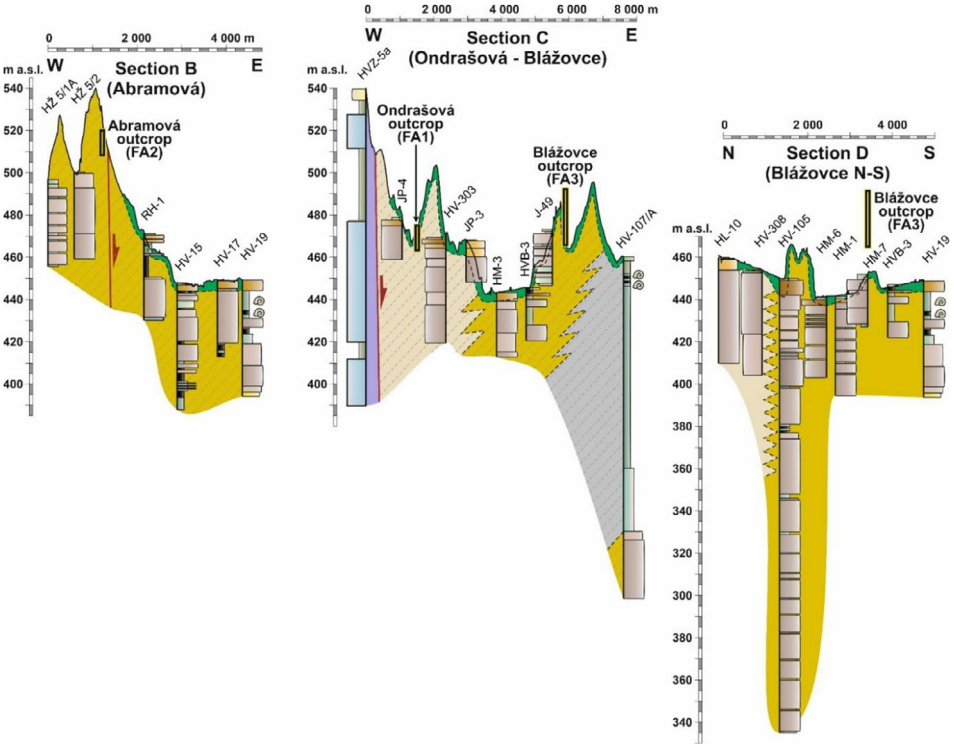

Fig. 3. Geological sections depicting borehole lithological profiles along the Abramová outcrop (Section B), along the line between Ondrašová and Blažovce outcrops in the west–east direction (Section C), and in perpendicular north-south direction along the Blažovce outcrop (Section D). The position of the outcrops is a projection perpendicular to the section line preserving the altitude of the stratigraphic section. A simplified version of the sections is present in [2]. Explanations in Fig. 5. Location in Fig. 1.

Table 1 (file "Statistical properties of lithofacies observed on the alluvial fan outcrops.xlsx"). The lithofacies assemblage is dominated by gravelly or sandy-gravelly tabular bodies, forming 80.3°% (Valča), 89.7°% (Ondrašová) and 80.8°% (Slovany) of the stratigraphic sections. The remaining proportions of the outcrops comprise tabular or lenticular bodies of sandy muds or muds reaching thickness generally below 30 cm.

The file "An aerial image (GoogleEarth) and Lidar digital elevation model of the Blažovce gravel quarry, showing position of the outcrop walls.jpg" indicates a detailed position of outcrop walls within the Blažovce site quarry. Orientation of fan delta foresets was measured from bottom to top of the quarry and the results are included in the file "Measurements of orientation of fan delta foresets and their basal surfaces from the Blažovce site.xlsx". The foreset orientation results are also visualised in Fig. 6 (file "Visualization of orientation of the fan delta foreset planes and their basal surfaces from the Blažovce site.jpg"). The southwest direction is prevailing, while it ranges from west to south-southeast.

The file "Correlation of Martin - claypit outcrops in Pipík (2004) Mineralia Slovaca 36, 87–100, and in Šujan et al. (2023) Palaeogeography, Palaeoclimatology, Palaeoecology 628, 111746.jpg" aims to indicate the correlation of the outcrop recently investigated at the Martin – claypit site [2] with the outcrop investigated by [5]. The file A sketch of stratigraphy at the Turčianske Kľačany – Kúdel outcrop.jpg" indicates stratigraphic observations at the Turčianske Kľačany – Kúdel site and position of the sampling points.

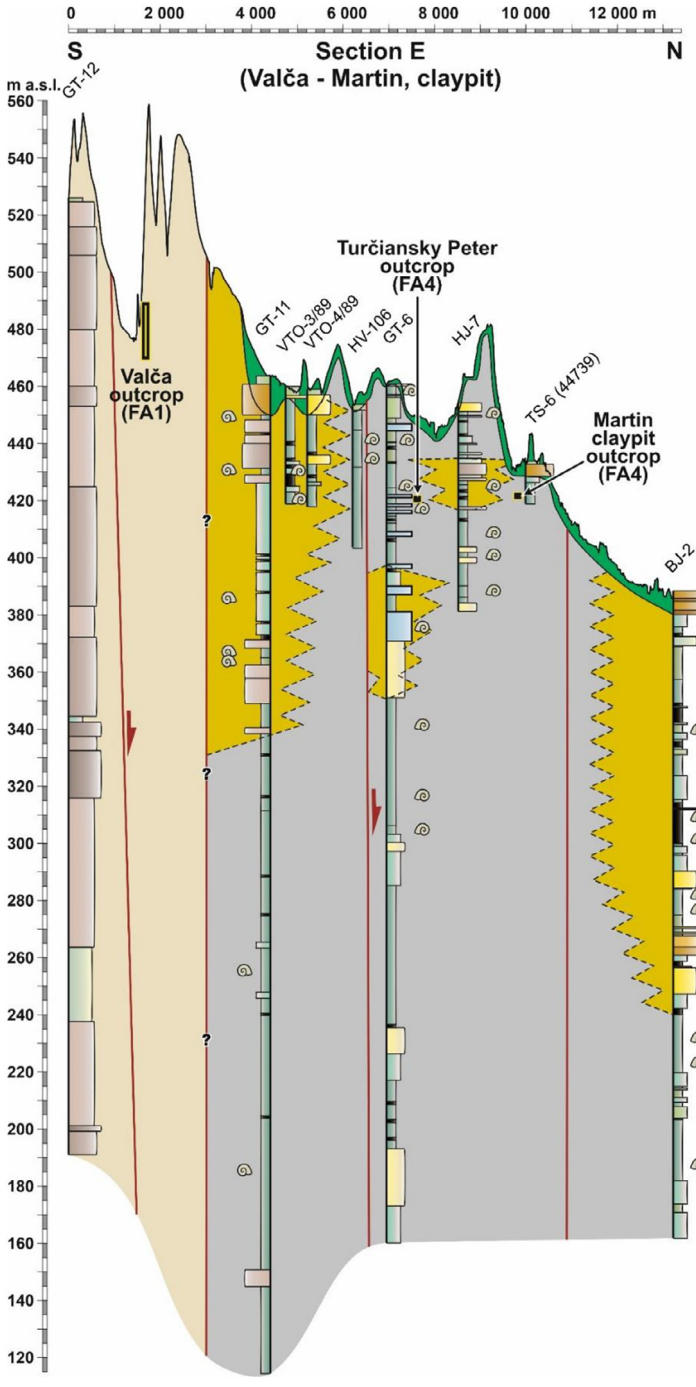

Fig. 4. Geological section depicting borehole lithological profiles along the line between Valča, Turčiansky Peter and Martin - claypit outcrops. The position of the outcrops is a projection perpendicular to the section line preserving the altitude of the stratigraphic section. A simplified version of the section is present in [2]. Explanations in Fig. 5. Location in Fig. 1.

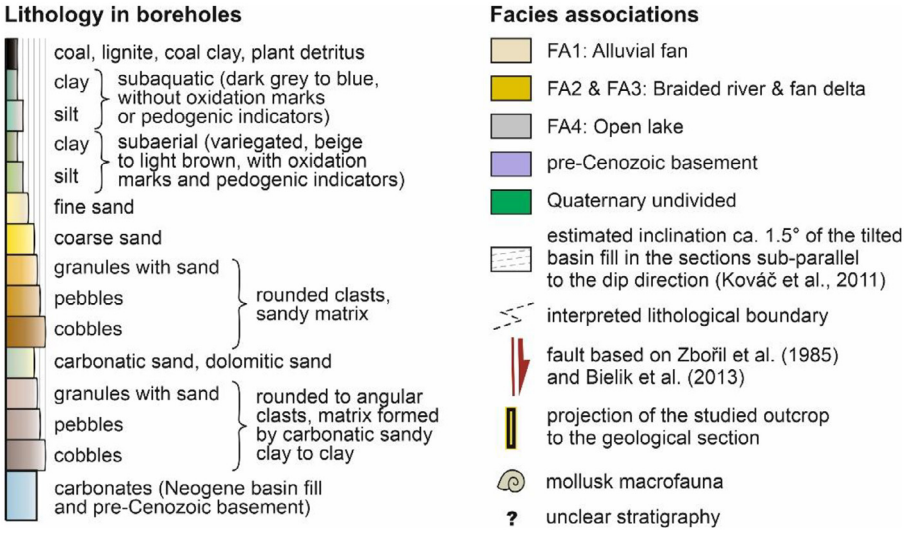

Fig. 5. Explanations for lithological profiles of boreholes and for facies associations in Figs. 2–4.

Table 1
Statistical properties of lithofacies observed on the alluvial fan outcrops. See file "List of lithofacies documented on the outcrops in the Turiec Basin.xlsx" for explanation of lithofacies codes.

Outcrop	Lithofacies	Proportion (%)	Abundance (n)	Average thickness AT (m)	Maximum thickness (m)	Minimum thickness (m)
Valča	Gm. Gsm. Sm	21.7	16	0.27	0.61	0.06
	Gmg	12.8	2	1.25	1.48	0.83
	Gmgr	7.2	1	1.41	1.41	1.41
	GFp	38.6	8	0.95	1.50	0.27
	FSm. Fm	15.9	17	0.18	0.53	0.07
	FSl	3.8	5	0.15	0.30	0.06
Ondrašová	GSm. Gm	89.7	18	0.98	3.15	0.06
	FSm. Fm	6.2	9	0.09	0.13	0.05
	Fl	4.1	3	0.18	0.26	0.10
Slovany	Gm	38.3	5	0.63	1.38	0.25
	Gmgr	42.5	2	1.75	2.00	1.48
	FSm. Fm	12.2	3	0.34	0.80	0.09
	FSl	7.0	3	0.19	0.31	0.12

2.3. Granulometry

Selected examples of gravelly lithofacies from alluvial fan and fan delta strata underwent grain size analysis by sieving with resulting data in the file "Granulometry - sieving of gravelly samples.xlsx". The values are depicted in Fig. 7 and evaluated by gain size parameters according to [8] in Table 2, namely the mean grain size, sorting, asymmetry, and kurtosis. The photographs of the gravel grain size classes, separated by sieving, show the level of rounding and lithological appearance of samples taken from all three alluvial fan sites and from the fan delta site Blažovce (.jpg files in the folder "Photo documentation of grain size classes for the gravelly samples taken from the Turiec Basin"). The grain size distribution of muddy strata from the Blažovce site was assessed by laser diffraction. Measured data are included in separate .xls files of the folder "Laser diffraction results" and the histograms of distribution within the grain size classes are depicted in Fig. 8.

Table 2
Grain size parameters of the samples analyzed by laser diffraction and sieving. Parameters calculated according to [8].

Laser diffraction grain size analysis of muddy samples								
Phi unit	Blaž-1 (Fh)	Blaž-2 (Fh)	Blaž-3 (Fm)	Blaž-4 (Fm)	Blaž-5 (Fm)	Blaž-6 (FSh)	Blaž-7 (Fh)	Blaž-X (FSh)
Mean (first moment)	6.746	6.704	6.890	6.699	6.891	6.320	6.702	5.400
Sorting (second moment)	1.277	1.083	1.362	1.502	1.433	1.549	1.278	1.615
Asymmetry (third moment)	−0.212	0.293	−0.241	−0.721	−0.151	−0.238	−0.253	0.599
Kurtosis (fourth moment)	2.863	2.504	3.190	3.943	3.290	3.136	3.127	3.036
Classification								
Mean (first moment)	Fine silt	Fine silt	Fine silt	Fine silt	Fine silt	Fine silt	Fine silt	Medium silt
Sorting (second moment)	Poorly sorted	Poorly sorted	Poorly sorted	Poorly sorted	Poorly sorted	Poorly sorted	Poorly sorted	Poorly sorted
Asymmetry (third moment)	Negative	Positive	Negative	Negative	Negative	Negative	Negative	Positive
Kurtosis (fourth moment)	Leptokurtic	Leptokurtic	Leptokurtic	Leptokurtic	Leptokurtic	Leptokurtic	Leptokurtic	Leptokurtic

Sieving grain size analysis of gravelly-sandy samples								
Phi unit	Slov-K-1 (Gm)	Blaz-K-1 (Gmm)	Blaz-K-2 (Gh-for)	Blaz-K-3 (Gt)	Val-K-1 (Gm)	Val-K-2 (GFp)	Ondr-K-1 (GSm)	Ondr-K-2 (Gm)
Mean (first moment)	−1.218	−1.737	−0.937	−2.994	−1.671	0.175	0.153	−0.749
Sorting (second moment)	3.285	3.198	3.266	2.369	3.110	3.142	3.437	3.129
Asymmetry (third moment)	0.610	0.936	0.477	2.121	0.866	0.151	0.028	0.429
Kurtosis (fourth moment)	1.864	2.358	1.785	6.366	2.383	1.401	1.316	1.840
Classification								
Mean (first moment)	Granule	Granule	Very coarse sand	Pebble	Granule	Coarse sand	Coarse sand	Very coarse sand
Sorting (second moment)	Very poorly sorted	Very poorly sorted	Very poorly sorted	Very poorly sorted	Very poorly sorted	Very poorly sorted	Very poorly sorted	Very poorly sorted
Asymmetry (third moment)	Very positive	Very positive	Very positive	Out of the range	Very positive	Positive	Symetric	Very positive
Kurtosis (fourth moment)	Leptokurtic	Leptokurtic	Leptokurtic	Out of the range	Leptokurtic	Leptokurtic	Leptokurtic	Leptokurtic

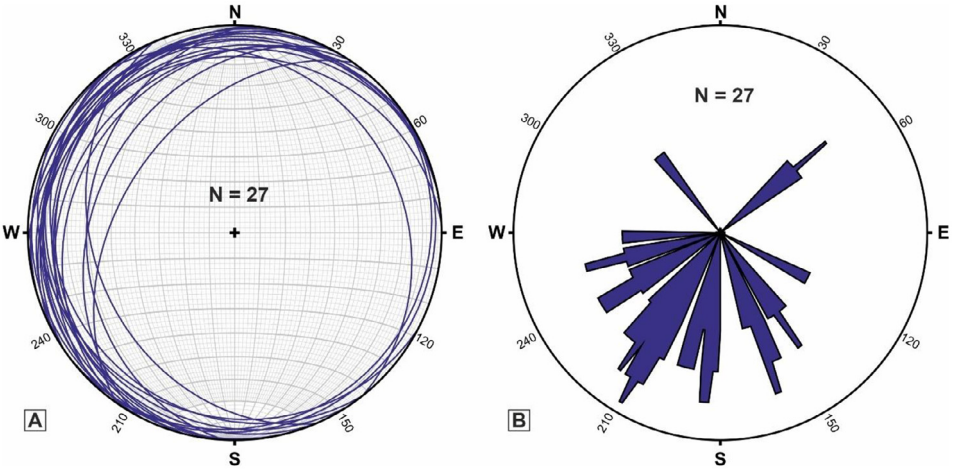

Fig. 6. Visualization of orientation of the fan delta foreset planes and their basal surfaces based on the Table 3. A. Stereographic projection created using the Stereonet software [6]. B. Rose diagram created using the MARD application [7].

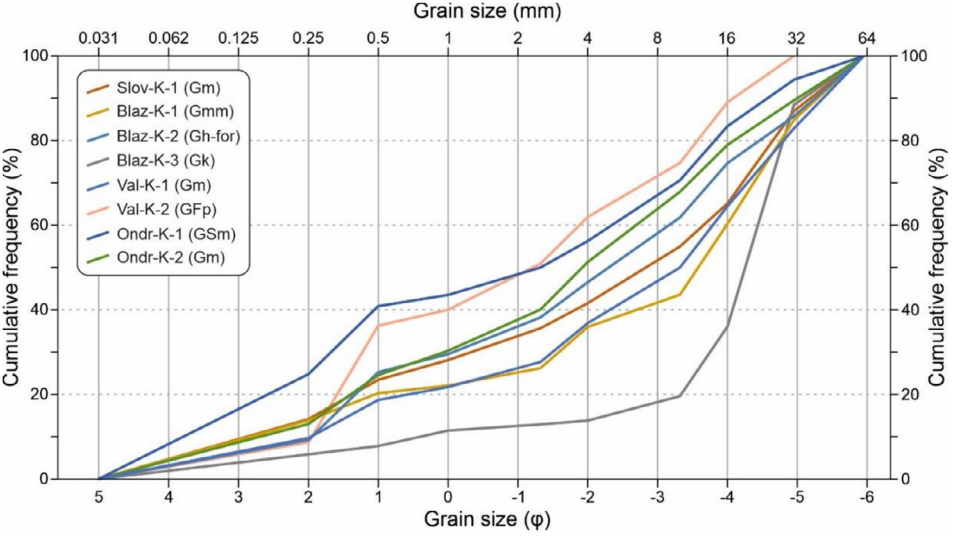

Fig. 7. Grain size cumulative curves obtained by sieving of gravelly samples from the Turiec Basin outcrops. Lithofacies indicated in brackets are explained in the file "List of lithofacies documented on the outcrops in the Turiec Basin.xlsx".

2.4. Geochemistry

Whole rock XRF analysis results of representative muddy samples from 12 sites (sample per site, except Slovany) are included in the file "Geochemistry - raw XRF, ICP-ES and ICP-MS data.xlsx". Additionally, the same file includes the results of whole rock analysis of five muddy samples taken from the Blažovce site, performed using ICP-ES (major elements) and ICP-MS (trace elements). The elemental concentrations served for calculation of geochemical indexes according to [9], included in the Tables 3 and 4. This includes SiO_2/Al_2O_3, Si/Al, K_2O/Al_2O_3, CIA, Fe/Al, $Fe_{(ef)}$, $V_{(ef)}$, $P_{(ef)}$, $Ba_{(ef)}$, $Mn_{(ef)}$, $Al_{(ucc)}$, CaO_{mol} and MgO_{mol}.

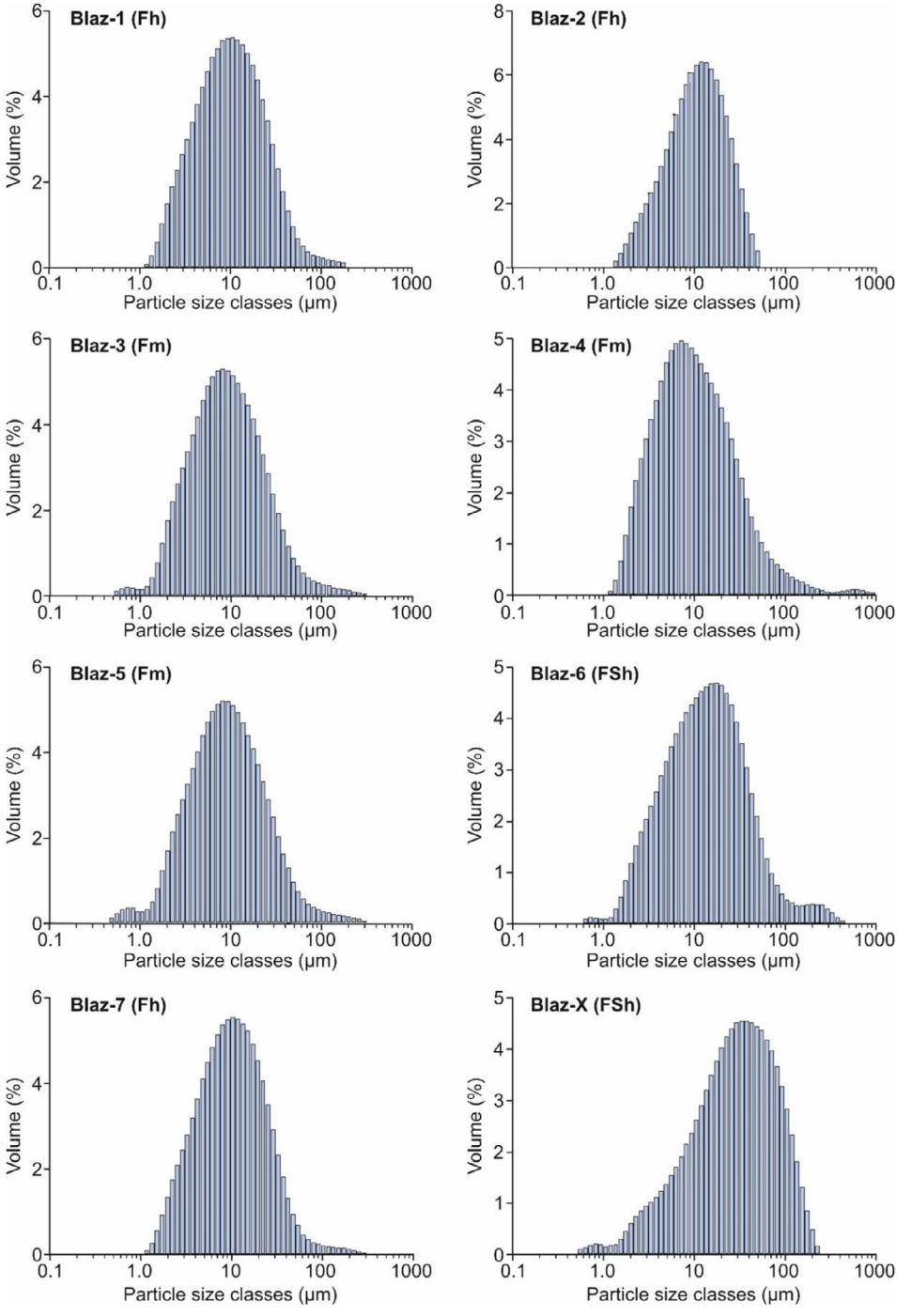

Fig. 8. Particle size distributions of samples from the Blažovce site. The samples Blaz-1 to Blaz-7 are identical with the samples analyzed for the authigenic $^{10}Be/^{9}Be$ dating.

Table 3
Geochemical indexes calculated according to [9] from XRF data measured from selected representative samples from all studied sites (Table 6).

Sample	Type		SiO_2/Al_2O_3	Si/Al	K_2O/Al_2O_3	CIA	Fe/Al	Fe(ef)	V (ef)	P(ef)	Ba(ef)	Mn(ef)	Al(ucc)	CaO mol	MgO mol
ValLom-1	alluvial fan	Dated sites	2.19	1.93	0.18		0.31	0.71				0.00	0.18	0.66	0.37
Ondr-1	alluvial fan		2.12	1.87	0.15		0.09	0.21	3.35	3.19		0.00	0.37	0.57	0.35
Kolisky-3	braided river		2.38	2.10	0.14		0.40	0.92	3.01			0.51	0.49	0.60	0.16
SocKos-1	braided river		2.72	2.40	0.21		0.50	1.15				0.58	0.38	0.57	0.15
Blaz-3	fandelta		2.08	1.83	0.15		0.27	0.62				0.18	0.77	0.37	0.15
MarTeh-1	open lake		3.43	3.03	0.22	73.49	0.27	0.63				0.56	0.72	0.13	0.05
TurPet-1	open lake		3.02	2.67	0.22		0.34	0.77				1.52	0.81	0.09	0.05
Kudel-1	open lake		3.74	3.31	0.23	67.78	0.30	0.68				0.40	0.59	0.15	0.05
MalCep-3	river terace	Initial autigenic	3.16	2.79	0.14		0.39	0.89			0.71	0.48	0.79	0.14	0.10
VelCep-2	alluvial fan	$^{10}Be/^{9}Be$ ratio	2.51	2.22	0.11		0.40	0.92			0.85	0.43	1.05	0.02	0.04
Kalam-Q-1	poorly drained floodplain	sites	3.50	3.09	0.17	71.92	0.58	1.32		4.10	1.61	3.40	0.70	0.02	0.02
Kost-Q-1	well drained floodplain		3.31	2.92	0.19	75.84	0.32	0.74		1.91	0.95	0.84	0.81	0.02	0.04

Table 4
Geochemical indexes calculated according to [9] from ICP-ES and ICP-MS data measured from fan delta muddy samples of the Blažovce site (Table 8).

Sample	MDL Type	CO_2 wt. %	SiO_2/Al_2O_3	Si/Al	K_2O/Al_2O_3	CIA McLennan	Fe/Al	Corg/P molar ratio	U (ef)	Ni (ef)	Co (ef)	Fe(ef)	V (ef)	P(ef)	Mo(ef)	Ba(ef)	Mn(ef)	Cu(ef)	As(ef)	Al(ucc)
									Normalisation to UCC (McLennan 2001)									44.01	56.08	40.03
Blaz-1	fandelta	17.88	2.06	1.82	0.13	86.24	0.40	54.87	1.41	0.82	0.31	0.91	1.27	0.46	0.78	0.34	0.00	0.41	0.23	0.24
Blaz-2	fandelta	16.20	2.12	1.87	0.13	86.38	0.41	33.24	1.20	0.56	0.32	0.94	1.23	0.51	0.88	0.34	0.00	0.37	0.20	0.22
Blaz-3	fandelta	16.97	2.27	2.00	0.14	85.86	0.25	50.82	1.28	0.26	0.33	0.58	1.26	0.33	0.14	0.40	0.41	0.39	0.22	0.23
Blaz-5	fandelta	24.26	2.28	2.01	0.12	87.39	0.28	63.82	1.10	0.32	0.44	0.65	1.10	0.46	0.39	0.37	0.38	0.55	0.43	0.17
Blaz-7	fandelta	22.61	2.51	2.22	0.18	82.77	0.21	56.73	1.70	0.18	0.19	0.49	1.17	0.43	0.18	0.38	0.00	0.51	0.28	0.29

2.5. Mineralogy

The folder "Mineralogy" includes results obtained by XRD analysis of the corresponding 12 samples, which underwent also the XRF investigation. The results show analogical trends in comparison to the geochemical analyzes (file "Quantitative mineral composition of whole rock sample and semi-quantitative mineral composition of the below 2 μm fraction obtained by XRD.xlsx"). Fig. 9 (file "XRD patterns of whole rock samples.jpg") mirrors the XRD record of the specific samples, while the file "Oriented XRD patterns of fraction below 2 μm after treatment for identification, sample Ondr-1.jpg" serves as an example of the XRD record of the fraction <2 μm. The annotated diffraction maximums in the figure indicate the content of low charge vermiculite/high charge smectite and smectite, illite and kaolinite. It does not intercalate with DMSO and kaolinite which forms intercalation compounds with DMSO, and finally also dolomite is indicated.

2.6. Geochronology - Authigenic $^{10}Be/^{9}Be$ Dating

2.6.1. Sample processing

The folder "Sample processing" includes sheets with all weights measured during analytical process of the authigenic phase extraction (e.g., weight of the crushed sample, weight of tubes and bottles used), which preceded the column chromatography. The data allow for a recalculation of all the beryllium isotope results provided by [2].

2.6.2. Isotopic measurement and age data

The file "Concentrations of ^{9}Be and ^{10}Be, natural ^{10}Be-^{9}Be ratios and authigenic ^{10}Be-^{9}Be ages for the analyzed samples, calculated using five initial ratios (N_0) determined in the Turiec Basin.xlsx" in the folder "Isotopic measurement and dating results" includes the concentrations beryllium isotopes based on accelerator mass spectrometry and ICP-MS measurements, natural $^{10}Be/^{9}Be$ authigenic ratios, and the authigenic $^{10}Be/^{9}Be$ ages calculated using five independently determined initial ratios from the Late Pleistocene to Holocene sites and a back-calculated paleo-initial ratio using the SLPR-1 borehole core, all located in the Turiec Basin [2]. The isotopic ratios of the 31 dated samples range from $0.87 \pm 0.06 \times 10^{-11}$ to $56.62 \pm 1.65 \times 10^{-11}$. The uncertainty of the radiometric ages propagate from the errors of the initial ratio, analytical error of the isotopic ratio and the uncertainty of the ^{10}Be decay constant. Hence, the within-site variability is more reasonable to evaluate using the radiometric ages. Irrespective of the selected initial ratio, the ages of dated sites overlap within uncertainties, except of the four outliers: Kolisky-2, Blaz-1, Blaz-4, Kudel-3.

Depending on the selected initial ratio, the ages attain distinct values. The highest difference of 3.90 Myr is attained between Veľký Čepčín and Košťany initial ratios, and the lowest one 0.93 Myr between Košťany and Kaľamenová initial ratios. The youngest ages are provided by the Veľký Čepčín initial ratio and range from 4.149 ± 0.162 Ma to 10.193 ± 0.837 Ma (excluding outliers). The oldest age range from 8.050 ± 0.157 Ma to 14.095 ± 0.830 Ma is provided by the Košťany initial ratio. The reasoning for selection of initial ratio and usage of specific ages is explained in [2].

2.7. Strontium isotopes

Since the presentation of strontium isotope data in [10,11] does not allow to observe the specific position and stratigraphic context of the sampling points, essential for evaluation of their spatial and temporal variability, the data are summarized in the file "Strontium isotope measurement results from Pipík et al. (2012) Journal of Paleolimnology 47, 2, 233-249.xlsx" in the folder "Strontium isotopes". Additionally, the position of the 16 strontium isotope samples is depicted in Fig. 10 together with a chart, allowing to observe the variability across the Turiec Basin

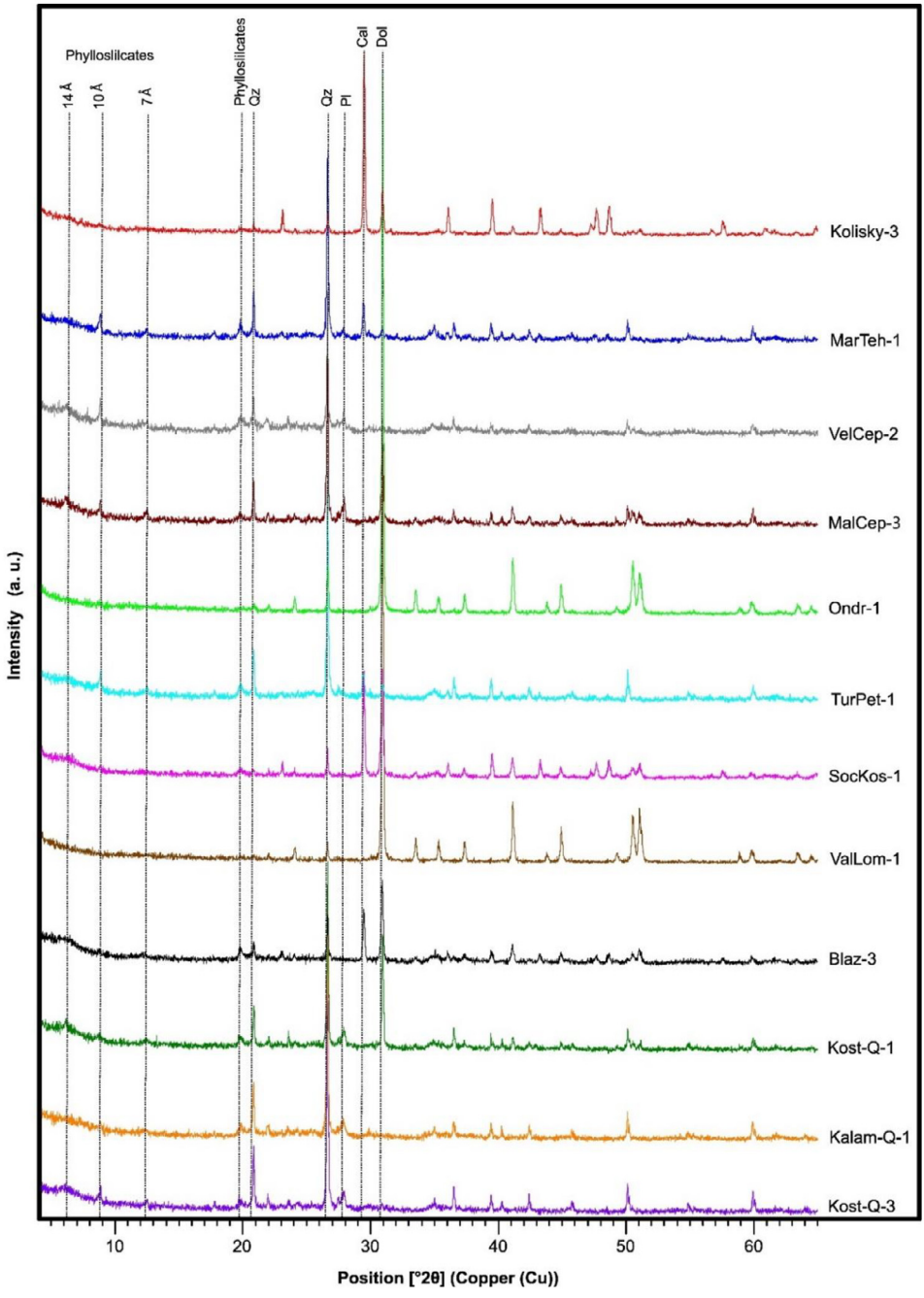

Fig. 9. XRD patterns of whole rock samples. Abbreviations: Qz – quartz; Pl – plagioclase; Cal – calcite; Dol – dolomite.

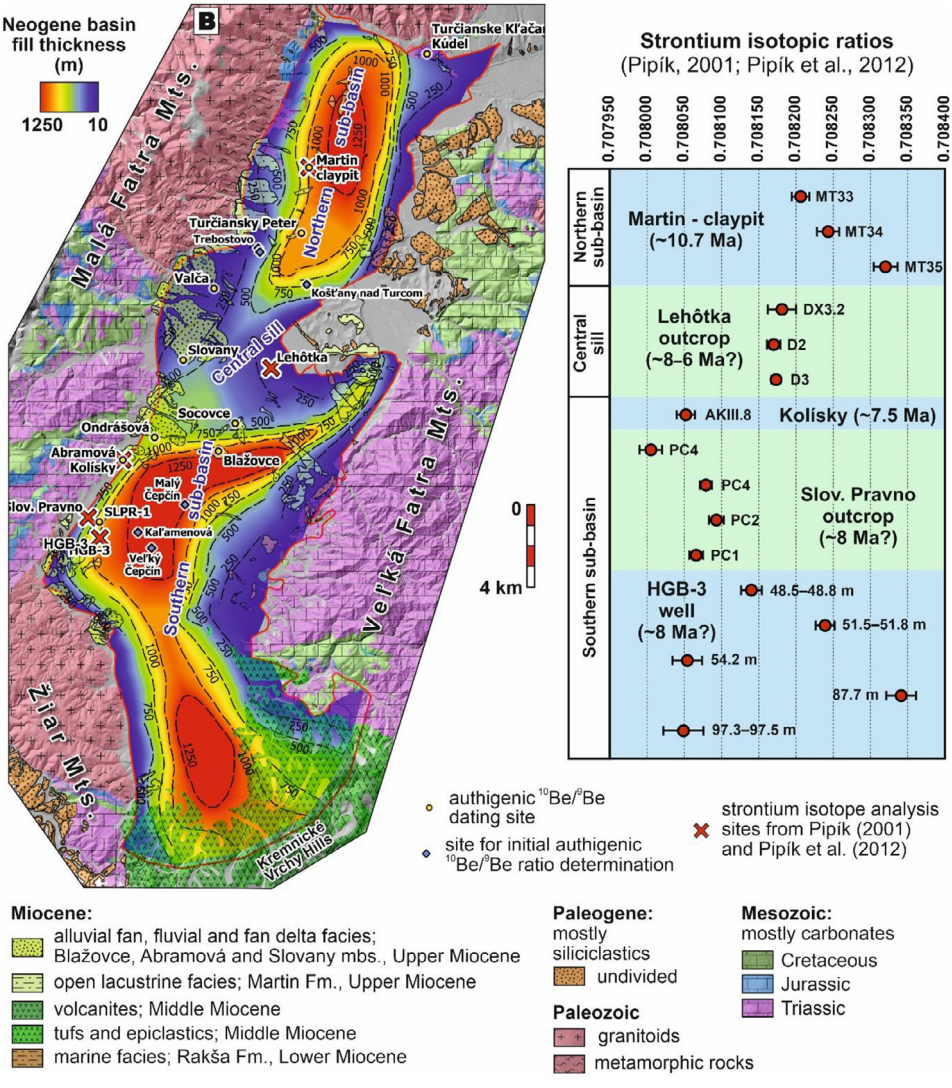

Fig. 10. Simplified geological map of the Turiec Basin according to [12] with thickness of the Neogene basin fill based on [4], showing location of the sites sampled for strontium isotopic analyzes by [10,11]. The map is modified from [2]. The Sr isotopic analysis results included in these studies are shown in the table on the right.

in comparison to the sites investigated in [2]. The age estimates of the sites are based on [2]. Following values were measured by [10,11]:

- Three samples in the northern sub-basin (Martin – clapit outcrop) yielded the range 0.708206–0.70832;
- Central sill is represented by the three samples (Lehôtka outcrop) in the range 0.7081699–0.708181;
- The southern sub-basin was investigated with 10 samples (HGB-3 borehole, Abramová Kolísky outcrop, Slovenské Pravno outcrop) with a relatively extensive range of 0.708079–0.708341. The high variability is observed especially in the borehole core HGB-3.

3. Experimental Design, Materials and Methods

3.1. Stratigraphy in borehole profiles

Lithology of the sedimentary succession in the vicinity of the outcrops (investigated by [2]) was examined using a dataset of 45 borehole lithological logs with depths ranging from 20 m to 900 m and with an average depth of 98 m. The logs were acquired from 18 final reports, listed in the file "List of final reports including the boreholes used for the geological sections.xlsx". The reports are stored in the Geofond archive of the State Geological Institute of Dionýz Štúr, available online at https://da.geology.sk/navigator/?desktop=Public. The boreholes were performed for various types of geological prospection, including hydrogeology, geothermal and ore geology prospection and general geological research for mapping. The precision of the lithological descriptions depends on the coring method and the gained data were only suitable to indicate different sedimentary units at the scale of 0.5 m. The lithology was unified using a code of 15 lithological classes, considering the dominant grain size, the character of the sediment matrix and rounding in the case of gravelly lithotypes. The presence or absence of oxidation and pedogenic marks as well as variegated color in contrast to blue to dark grey color was used to distinguish subaerial and subaquatic muddy lithotypes. The fault network indicated by [4,12] was considered during construction of the geological sections. Topography for the geological sections is based on the Lidar DEM model provided by the Geodesy, Cartography and Cadaster Authority of the Slovak Republic. A dip of 1.5° of the Upper Miocene basin fill towards the western margin of the basin was published by [13], and was included in the sections oriented generally in the corresponding direction.

3.2. Sedimentology

The sedimentological research was performed using standard facies analysis, logging and documentation of facies distribution by outcrop schemes [14]. The facies were identified on outcrops using visual evaluation of grain size, structure, texture, geometry and size of the strata. Facies analysis was applied to nine outcrops, comprising quarries (Abramová, Ondrašová, Blažovce, Valča and Slovany sites), cuts on the river and creek banks (Turčiansky Peter, Turčianske Kľačany – Kúdel sites), a natural cliff (Socovce site) and a gully nearby the Martin abandoned claypit, which is presently a landfill. Paleotransport orientation was investigated by measuring the orientation of bedding planes of fan delta foresets and their basal surface using a geological compass, attaining 27 measurements from the Blažovce site.

3.3. Granulometry

Grain size of the alluvial fan and fan delta deposits was further investigated by sieving of selected gravelly samples with the sieves of the size 0.25 mm, 0.5 mm, 1.0 mm, 2.5 mm, 4.0 mm, 10.0 mm, 16.0 mm, 31.0 mm and 64.0 mm (depicted in the folder "Photo documentation of grain size classes for the gravelly samples taken from the Turiec Basin"). Each grain size class was visually evaluated according to the clast roudness. Laser diffraction grain size analysis was applied to eight muddy samples using Malvern Mastersizer 3000 facility at the Institute of Geological Sciences, Jagiellonian University in Krakow, Poland. Percentual proportion of grains in 97 particle size classes between 0.01 µm and 2000 µm fractions was determined. Histograms of particle size classes were constructed for each sample.

3.4. Geochemistry

Twelve samples were selected for the whole rock geochemical analysis by X-ray fluorescence, each sample representing a single site. Eight samples were taken from the outcrops of the

Miocene basin fill, which were analyzed also using sedimentology and the authigenic $^{10}Be/^{9}Be$ dating. In order to compare the paleoenvironmental conditions of the sites selected for the initial $^{10}Be/^{9}Be$ ratio determination with the dated sites, another four samples were taken from the initial ratio sites.

The specimens were ground into powder, and a mixture of 5 g of material with 1 g of cellulose was prepared. Subsequently, the combination was compacted into pellets using an automated apparatus applying a pressure of 160 kN. The X-ray fluorescence (XRF) measurements were conducted at the Slovak National Museum laboratory in Bratislava, Slovakia, utilizing the ARL Quant'X (Thermo Scientific Inc, USA) energy-dispersive X-ray fluorescence spectrometer. The excitation rays were generated via an air-cooled X-ray tube (with a rhodium anode, maximum power of 40 W, anode voltage ranging from 4 to 50 kV, and anode current varying from 0.02 to 1.98 mA). The emitted X-rays were detected employing a Peltier-cooled Si (Li) detector (with a crystal area of 15 mm2 and crystal depth of 3.5 mm, exhibiting an energy resolution of 155 eV at the 5.9 keV Mn Kα line), along with a pulse processor. To correct the matrix and calibrate the XRF data processing, Uniquant software (Ver 5.46) was utilized, relying on a series of fundamental parameters and distinct algorithms provided by Thermo Fisher Scientific. The integration of certified reference materials (NSC DC73043, CRM016-50, BCR-176R, and BCR-320R) with the Uniquant data processing was also undertaken. Notably, all measurements were executed under vacuum conditions.

Chemical information for five samples of muddy substances extracted from the deltaic sediments was procured through inductively coupled plasma emission spectrometry (ICP-ES, for major oxides) and inductively coupled plasma mass spectrometry (ICP-MS, for trace elements) at the Bureau Veritas mineral laboratories situated in Vancouver, Canada. The pulverized samples were dissolved via Lithium Borate Fusion. Rigorous quality control was upheld via duplicate sample measurements, calibration using standard reference materials STD BVGEO01, STD DS11, STD OREAS262, and STD SO-19, as well as the use of blank samples. Additionally, the content of total organic carbon (TOC), carbon (C), and sulfur (S) was analyzed using the LECO Carbon–Sulphur analyzer.

3.5. Mineralogy

At the Croatian Geological Survey in Zagreb, Croatia, the X-ray diffraction (XRD) method was employed to analyze twelve samples of silty mud gathered from the corresponding outcrops, matching those examined via X-ray fluorescence (XRF). XRD patterns were captured using both random and oriented mounts of the <2 μm fraction and entire rock samples with the PANalytical vertical goniometer (type X'Pert), equipped with a Cu-tube. The experimental conditions encompassed a voltage of 45 kV, a current of 40 mA, a PW 3018/00 PIXcel detector, a primary beam divergence of 1/4°, and a continuous scan (step 0.02 °2θ/s).

The preparatory steps for the XRD assessments involved grinding the samples for overall rock analyses, sieving them through a 63 μm sieve to eliminate a part of the carbonate content, and then segregating the <2 μm fraction from the sample through a centrifugation process for the oriented mounts on glass slides. For the <2 μm fraction, an array of treatments were applied, including air drying, solvation with ethylene-glycol, saturation with K^{+} and Mg^{2+}, and various combinations of solvation with ethylene-glycol, dimethyl sulfoxide (DMSO), or glycerol, in conjunction with K^{+} or Mg^{2+} saturation. Moreover, selected samples were subjected to temperatures exceeding 400 °C for over half an hour.

The identification of clay minerals was conducted based on the alterations in the XRD patterns after the diverse treatments proposed by Starkey, Blackmon, and Hauff [15] and Moore and Reynolds [16]. The X-ray interpretation was executed using the High Score Plus [17] calculation and the database provided by the International Centre for Diffraction Data [18].

3.6. Authigenic $^{10}Be/^{9}Be$ dating

The samples for authigenic $^{10}Be/^{9}Be$ were taken from natural and artificial exposures by digging several decimeters deep into the wall. The samples consisted of ~100 g of clean, muddy sediment. Visual inspection was done to avoid material affected by recent weathering and pedogenic processes. Samples were stored in plastic bags. Processing started with drying and crushing in an agate mortar. All weighting was performed using the Ohaus PA224C with the precision of 0.1 mg. All used chemicals were of the *pro analysis* (p.a.) purity level.

Leaching of the authigenic phase was applied to a sample weighted in the range of 2.2450–2.2550 g. The leaching solution consisted of 0.04 M NH_2OH-HCL in a 25 % acetic acid, and a volume of 45 ml (20-times the weight of a sample) was applied per sample to a 50 ml tube. The process of sequential leaching was developed by [19,20] to prevent contamination of the authigenic phase leachate by beryllium from the mineral lattice of the sediment grains. Each tube included a magnet for magnetic stirring and was positioned in a sand bath with a temperature of ~90–95 °C. The leaching process took 6 h, followed by centrifugation to separate the leaching solution from the residual sediment. The residual sediment was cleaned three times by additional 10 ml of leaching solution by vortexing and subsequent centrifugation, and trashed.

An aliquot for beryllium concentration measurements with the volume of 2 ml was taken from the resulting ~75 ml of the leaching solution. Total beryllium concentrations were measured from the aliquots by inductively coupled plasma mass spectrometry (ICP-MS) using the PlasmaQuant ICP-MS System (Analytik Jena AG) facility at the Chemical Institute of the Slovak Academy of Sciences (Hlohovec, Slovakia). The aliquots underwent precipitation to dryness in small 25 ml beakers, followed by dissolution in ~2 ml of 5 % nitric acid, added into 8 ml of demineralized water, resulting in 10 ml of solution. This solution was subsequently used to prepare sub-samples with standard additions to overcome the matrix effect during ICP-MS measurements using linear regression. The aliquots were additionally analyzed for the concentration of Fe, Mn and Al by the same ICP-MS facility.

Ca. 450 µg of the Scharlau commercial ICP beryllium standard was added to the remaining solution for the following steps of beryllium purification. The $^{10}Be/^{9}Be$ ratio of this specific bottle of standard was measured to reach ~$7–8 \times 10^{-15}$ [21]. The solution was evaporated, and a precipitate was formed after adjusting pH to 8–9 by the use of ammonium hydroxide. The precipitate was then dissolved in 1 ml of 10.2 M HCl. The column chromatography approach according to [22] was then applied, using the resins Dowex 1x×8 and Dowex 50Wx8 in 8 cm high columns to separate beryllium from other elements present in the authigenic phase. A precipitate was formed again by adjusting pH to 8–9 by adding few drops of ammonium hydroxide. The precipitate was cleaned two times by water with pH ~8 in order to remove NH_4Cl. Aging of a precipitate after each vortexing step was included in the workflow to achieve low sample losses [23]. The cleaned precipitate was dissolved in few drops of nitric acid and transferred to crucibles. After 30 min of heating at ca. 300 °C on a hotplate, the crucibles were placed in an oven and samples were oxidized at 800°C for an hour. Finally, BeO was mixed with niobium powder, pressed into copper cathodes and delivered for accelerator mass spectrometry at the French national AMS facility ASTER [24].

3.7. Strontium isotopes

The strontium isotopic data were taken from [10,11] and depicted in Fig. 10, for the purpose to allow the temporal and spatial variability in the context of newly performed research in [2]. Sr isotopic composition ($^{87}Sr/^{86}Sr$) was measured by the authors of [10,11] on ostracode valves and mollusc shells. The shell fauna was analyzed using SEM to determine the extent of diagenetic shell alteration and identify the best fossils for Sr analyses. One to three ostracode valves, each valve weighing between 20 and 60 µg, were dissolved in 2 M HCl. Ion exchange chromatography was applied to these solutions to extract Sr. The same method was used for extraction of Sr

from small fragments of mollusc shells. Sr was loaded on Ta-activated W single filaments and $^{87}Sr/^{86}Sr$ data were measured on a fully automated Isomass VG54E mass spectrometer, using a SRM987 standard for reference [9].

Limitations

The relevance of borehole lithological logs could be biased by the arbitrary placement of the borehole locations due to a specific purpose of the surveys, hence, the boreholes are not dispersed homogeneously across the depicted basin.

The location of the sedimentological profiles and sampling points for dating relies on the availability of outcrops in the Turiec basin, which are mostly artificial. Therefore, the sedimentological and age data are not distributed homogeneously across the area.

Ethics statement

The authors have read and follow the ⟨13:italic ⟩ethical requirements⟨/13:italic⟩ for publication in Data in Brief and confirm that the current work does not involve human subjects, animal experiments, or any data collected from social media platforms.

Data Availability

Data for stratigraphic, granulometric, geochemical and authigenic 10Be/9Be geochronological analysis of Upper Miocene outcrops in the Turiec Basin, Western Carpathians (Central Europe) (Original data) (Mendeley Data)

CRediT Author Statement

Michal Šujan: Conceptualization, Methodology, Data curation, Formal analysis, Investigation, Writing – original draft, Writing – review & editing, Supervision, Funding acquisition, Project administration; **Kishan Aherwar:** Data curation, Formal analysis, Investigation, Writing – original draft, Writing – review & editing; **Rastislav Vojtko:** Conceptualization, Formal analysis, Investigation, Writing – original draft, Writing – review & editing, Funding acquisition; **Régis Braucher:** Conceptualization, Methodology, Data curation, Investigation, Writing – original draft, Writing – review & editing; **Katarína Šarinová:** Conceptualization, Methodology, Data curation, Formal analysis, Investigation, Writing – original draft, Writing – review & editing; **Andrej Chyba:** Conceptualization, Methodology, Data curation, Formal analysis, Investigation; **Jozef Hók:** Conceptualization, Formal analysis, Investigation, Supervision; **Anita Grizelj:** Methodology, Investigation, Writing – original draft; **Radovan Pipík:** Formal analysis, Writing – original draft; **Bronislava Lalinská-Voleková:** Methodology, Investigation, Writing – original draft; **Barbara Rózsová:** Data curation, Investigation; **Aster Team:** Data curation, Investigation.

Acknowledgments

The study was supported by the Slovak Research and Development Agency (APVV) under contracts Nos. APVV-16-0121, APVV-20-0120 and APVV-21-0281 and by the Scientific Grant Agency of the Ministry of Education, Science, Research and Sport of the Slovak Republic and the Slovak Academy of Sciences (VEGA) under the contract No. 1/0346/20. The free availability of the Lidar DEM data owned by Geodesy, Cartography and Cadaster Authority of the Slovak Republic (ÚGKK SR) and distributed by the Geodetic and Cartographic Institute, Bratislava (GKÚ) is acknowledged with gratitude.

Declaration of Competing Interest

The authors declare that they have no known competing financial interests or personal relationships that could have appeared to influence the work reported in this paper.

References

[1] M. Šujan, K. Aherwar, R. Braucher, K. Šarinová, A. Chyba, B. Lalinská - Voleková, R. Vojtko, Data for stratigraphic, granulometric, geochemical and authigenic $^{10}Be/^{9}Be$ geochronological analysis of Upper Miocene outcrops in the Turiec Basin, Western Carpathians (Central Europe), Mendeley Data V5 (2023), doi:10.1016/j.palaeo.2023.111746.

[2] M. Šujan, K. Aherwar, R. Vojtko, R. Braucher, K. Šarinová, A. Chyba, J. Hók, A. Grizelj, R. Pipík, B. Voleková, B. Rózsová, AsterTeam, application of the authigenic $^{10}Be/^{9}Be$ dating to constrain the age of a long-lived lake and its regression in an isolated intermontane basin: the case of Late Miocene Lake Turiec, Western Carpathians, Palaeogeogr., Palaeoclimatol., Palaeoecol. 628 (2023) 111746.

[3] M. Šujan, S. Rybár, M. Kováč, M. Bielik, D. Majcin, J. Minár, D. Plašienka, P. Nováková, J. Kotulová, The polyphase rifting and inversion of the Danube Basin revised, Glob. Planet. Change 196 (2021) 103375.

[4] L. Zbořil, J. Šefara, S. Halmešová, Geofyzikálny výskum Turčianskej kotliny, čiastková záverečná správa. Manuscript, Geofond Number: 60638, pp. 29 (in Slovak). Available online at: https://da.geology.sk/navigator/?desktop=Public, (1985).

[5] R. Pipík, Freshwater ostracods (Ostracoda) and Upper Miocene paleobiotopes of the northern part of the Turiec depression (Slovakia), Min. Slovaca (2004) 87–100 Slovak with English abstract.

[6] R.W. Allmendinger, Stereonet 11 - Versions 11.43 — 2022.08.12, dowloaded from https://www.rickallmendinger.net/stereonet, (2022).

[7] M.A. Munro, T.G. Blenkinsop, MARD—a moving average rose diagram application for the geosciences, Comput. Geosci. 49 (2012) 112–120.

[8] R.L. Folk, W.C. Ward, A study in the significance of grain-size parameters, J. Sediment. Petrol. 27 (1957) 3–26.

[9] S.M. McLennan, Relationships between the trace element composition of sedimentary rocks and upper continental crust, Geochem., Geophys., Geosyst. 2 (4) (2001), doi:10.1029/2000GC000109.

[10] R. Pipík, Les Ostracodes d'un lac Ancien et ses Paléobiotopes au Miocéne Supérieur: le Bassin de Turiec (Slovaquie), Thesis, Université Claude-Bernard, Lyon, 2001.

[11] R. Pipík, A.M. Bodergat, D. Briot, M. Kováč, J. Král, G. Zielinski, Physical and biological properties of the late Miocene, long-lived Turiec Basin, Western Carpathians (Slovakia) and its paleobiotopes, J. Paleolimnol. 47 (2) (2012) 233–249, doi:10.1007/s10933-011-9573-2.

[12] M. Bielik, M. Krajňák, I. Makarenko, O. Legostaeva, V.I. Starostenko, M. Bošanský, M. Grinč, J. Hók, 3D gravity interpretation of the pre-Tertiary basement in the intramontane depressions of the Western Carpathians: a case study from the Turiec Basin, Geol. Carpath. 64 (5) (2013) 399–408, doi:10.2478/geoca-2013-0027.

[13] M. Kováč, J. Hók, J. Minár, R. Vojtko, M. Bielik, R. Pipík, M. Rakús, J. Kráa, M. Åujan, S. Králiková, Neogene and quaternary development of the Turiec Basin and landscape in its catchment: a tentative mass balance model, Geol. Carpath. 62 (4) (2011) 361–379, doi:10.2478/v10096-011-0027-6.

[14] D.A. Stow, Sedimentary Rocks in the Field. A Colour Guide, Manson Publishing, London, 2005.

[15] H.C. Starkey, P.D. Blackmon, P.L. Hauff, The routine mineralogical analysis of clay-bearing samples, U.S. Geol. Surv. Bull. 1563 (1984) 1–31.

[16] D.M. Moore, R.C. Reynolds, in: X-ray Diffraction and the Identification and Analysis of Clay Minerals, Oxford University Press, Oxford, 1997, pp. 1–378.

[17] Panalytical B.V., X-pert high score plus software, The Netherlands, (2016).

[18] International Centre for Diffraction Data, PDF-4/Minerals, SN: MIND 220124-5612, https://www.icdd.com/pdf-4-minerals/, (2022).

[19] D. Bourlès, G.M. Raisbeck, F. Yiou, 10Be and 9Be in marine sediments and their potential for dating, Geochim. Cosmochim. Acta 53 (2) (1989) 443–452, doi:10.1016/0016-7037(89)90395-5.

[20] J. Carcaillet, D.L. Bourles, N. Thouveny, M. Arnold, A high resolution authigenic 10Be/9Be record of geomagnetic moment variations over the last 300 ka from sedimentary cores of the Portuguese margin, Earth Planet. Sci. Lett. 219 (3-4) (2004) 397–412, doi:10.1016/s0012-821x(03)00702-7.

[21] S. Merchel, R. Braucher, J. Lachner, G. Rugel, Which is the best 9Be carrier for 10Be/9Be accelerator mass spectrometry? MethodsX 8 (2021) 101486, doi:10.1016/j.mex.2021.101486.

[22] S. Merchel, U. Herpers, An update on radiochemical separation techniques for the determination of long-lived radionuclides via accelerator mass spectrometry, Radiochim. Acta 84 (4) (1999) 215–220, doi:10.1524/ract.1999.84.4.215.

[23] S. Merchel, S. Beutner, T. Opel, G. Rugel, A. Scharf, C. Tiessen, S. Weiß, S. Wetterich, Attempts to understand potential deficiencies in chemical procedures for AMS, Nucl. Instrum. Methods Phys. Res. Sect. B: Beam Interact. Mater. Atoms 456 (2019) 186–192, doi:10.1016/j.nimb.2019.05.005.

[24] M. Arnold, S. Merchel, D.L. Bourlès, R. Braucher, L. Benedetti, R.C. Finkel, G. Aumaître, A. Gottdang, M. Klein, The French accelerator mass spectrometry facility ASTER: improved performance and developments, Nucl. Instrum. Methods Phys. Res. Sect. B: Beam Interact. Mater. Atoms 268 (11–12) (2010) 1954–1959, doi:10.1016/j.nimb.2010.02.107.